EUROPEAN ORGANISATION FOR NUCLEAR RESEARCH

CERN-EP/85-35
March 18th, 1985

PRECISION MEASUREMENTS OF THE ELECTROWEAK MIXING-ANGLE

J. Panman

CERN

CH-1211 Geneva 23

Switzerland

Abstract: Low energy tests of the standard model and measurements of $\sin^2\theta$ are summarized. The status of new high precision determinations of the electroweak mixing angle using neutrino scattering are analysed and the precision is compared with direct measurements of the masses of the vector bosons W and Z at the CERN Sp$\bar{p}$S collider.

Talk given at the

First Aspen Winter Conference Series,

Aspen, CO, Januari 13-19 1985.

1. INTRODUCTION

After the discovery of the weak neutral-current [1] a lot of effort has been spent to test the prediction of the Glashow-Salam-Weinberg model that the coupling in all neutral-current phenomena depends on one single parameter, $\sin^2\theta$. Indeed, a unique value of this parameter can explain the couplings measured in many different processes, including leptonic and semileptonic neutrino scattering, asymmetries in electron-nucleon, electron-positron and muon-nucleon interactions, parity violating effects in atomic transitions, and the masses of the W and Z bosons.

This prediction is based on the Born approximation of the theory [2]. In the corrections to the Born terms different processes pick up different correction terms. Hence, measurements of $\sin^2\theta$ made with sufficient precision and extracted from the data using the simple zero-order approximations should show differences for different reactions. It is this feature which provides a test of the gauge nature of the theory.

The present status of measurements of $\sin^2\theta$ are briefly summarized in the first section. Then it is shown that the effects of first order corrections to the Born approximation are within reach of a new round of experiments. Some of the experiments aiming at such high precision measurements are described in some detail in the latter two sections.

2. LOW ENERGY TESTS

Many different experiments have been performed to test the low energy predictions of the theory. These tests include the weak isospin structure, the value of ρ, and the observation that $\sin^2\theta$ is process independent.

2.1 Isomultiplet structure and generation universality

The left-handed and right-handed isospin assignments, T^3_L and T^3_R, as postulated in the standard model and the resulting vector and axial vector couplings, g_V and g_A, are given in Table 1.

Table 1: Weak isospin assignments and couplings.

	T^3_L	T^3_R	g_A	g_V
ν	1/2	0	1/2	1/2
e,μ,τ	-1/2	0	-1/2	$-1/2+2\sin^2\theta$
u,c,t	1/2	0	1/2	$1/2-4/3\ \sin^2\theta$
d,s,b	-1/2	0	-1/2	$-1/2+2/3\ \sin^2\theta$

In determining the deviation from the standard model the left-handed isospin is taken from theory, and all deviations are attributed to a non-zero right-handed isospin value, predicted to vanish in the standard model. The results are summarized in Table 2 [3]. For the light quarks one has to add a systematic uncertainty of the size of the statistical one, since the result is obtained from a combined fit of many different processes.

No serious deviations from the model are found. This evidence confirms the isomultiplet structure of the model. By comparing the couplings of the

Table 2: Axial vector coupling and T^3_R determination.

	g_A	T^3_R
u	0.56 ± 0.02	-0.05 ± 0.02 ± syst.
d	-0.41 ± 0.04	-0.09 ± 0.04 ± syst.
s		$-0.6 < T^3_R < 0.3$ 90% c.l.
c	0.63 ± 0.20	-0.13 ± 0.20
b	-0.55 ± 0.13	0.05 ± 0.13
e	-0.51 ± 0.04	0.01 ± 0.04
μ	-0.52 ± 0.05	0.02 ± 0.05
τ	-0.44 ± 0.07	-0.06 ± 0.07

various generations one obtains good agreement, confirming the assumption of generation universality.

2.2 The value of ρ and $\sin^2\theta$

In many different processes a value of $\sin^2\theta$ was derived. According to the lowest order predictions of the standard model all these experiments should be described by a single value of the mixing angle. The experimental status is given in Table 3. From the table it is clear that at this level of precision no discrepancies have been found.

Another possible test of the standard model is the measurement of ρ. The ρ parameter describes the overall strength of the neutral-current (NC) with respect to the charged-current (CC) couplings. In the standard model ρ is equal to unity (to lowest order), and is a consequence of the symmetry breaking mechanism with doublets in the Higgs sector. Indeed experimental evidence favours values of ρ close to unity as shown in Table 3.

Table 3: Measurements of $\sin^2\theta$ and ρ.

process	$\sin^2\theta$	condition	ρ
νN	0.223±0.007±0.01	$\rho = 1$	1.01±0.02
eD	0.215±0.015±0.005	$\rho = 1$	
e^+e^-	0.18±0.02	$M(Z^0)$=93±2 GeV	1.17±0.09
$\nu_\mu e$	0.22±0.03±0.01	ρ indep.	1.09±0.14
μC	0.23±0.07±0.04	$\rho = 1$	
atomic parity violation	0.205±0.034±0.024	ρ indep.	
νp	0.182±0.023	$\rho = 1$	
W and Z masses	0.22±0.01	ρ indep.	1.00±0.036

3. NEXT TO LOWEST ORDER TESTS

The standard model, being based on gauge symmetries, is in principle calculable to all orders and its predictions can therefore be tested by experiment. One expects that effective values of $\sin^2\theta$ obtained in different processes are modified in a different way by higher order corrections. Therefore, these higher order corrections can be tested if sufficiently precise measurements of this parameter are available.

3.1 Direct mass measurements

The discovery of the intermediate vector bosons W and Z and a direct measurement of their mass at the Sp$\bar{p}$S collider [4] opens a new way of checking the standard model.

The relevant equations have been given in ref. [5]. The masses are given by

$$M(W) = A / \sin\theta \qquad M(Z^0) = 2A / \sin 2\theta \tag{1}$$

with $A = (37.2810 \pm 0.0003)$ GeV $/ \sqrt{(1-\Delta r)}$ and the correction term $\Delta r = 0.0696 \pm 0.0020$. By rewriting the equations one obtains a formula for $\sin^2\theta$ which is independent of the absolute calibrations of the mass measurement:

$$\sin^2\theta = 1 - M(W)^2 / M(Z^0)^2 \tag{2}$$

The radiative corrections can be measured by using

$$\Delta r = 1 - \frac{(37.2810 \text{ GeV})^2}{M(W)^2(1-M(W)^2/M(Z^0)^2)}$$

In the preceding equations ρ was taken from the standard model, if one releases this condition one obtains

$$\rho = \frac{M(W)^2}{M(Z^0)^2(1-A^2/M(W)^2)}$$

which can be compared with the measurement.

In Table 4 the results of the direct mass measurements are compared to the predictions of the model for $\sin^2\theta = 0.217 \pm 0.014$. Good agreement is observed at the level of accuracy of the experiments.

Table 4: Comparison with direct mass measurements.

quantity	UA1	UA2	standard model with $\sin^2\theta$ = 0.217 ± 0.014
M(W) (GeV)	80.9 ± 1.5 ± 2.4	83.1 ± 1.9 ± 1.3	83.0 +2.9 -2.7
$M(Z^0)$ (GeV)	95.6 ± 1.5 ± 2.9	92.7 ± 1.7 ± 1.4	93.8 +2.4 -2.2
$M(Z^0)$-M(W) (GeV)	14.7 ± 2.1 ± 0.4	9.6 ± 2.5 ± 0.2	10.8 ± 0.5
$\sin^2\theta$ eq.(2)	0.284 ± 0.035	0.196 ± 0.035	0.217 ± 0.014
Δr	0.252 ± 0.072 ± 0.045	0.051 ± 0.173 ± 0.030	0.0696 ± 0.0020
$\sin^2\theta$ eq.(1)	0.228 ± 0.008 ± 0.014	0.216 ± 0.010 ± 0.007	0.217 ± 0.014
ρ	0.928 ± 0.038 ± 0.016	1.006 ± 0.043 ± 0.01	1.00

3.2 Future improvements

Although many tests have been performed, none of them has yet reached sufficient precision to determine the validity of the first-order corrections. In order to recall the situation one sees that

$$\Delta r = 0.0696 \Rightarrow \Delta(M(Z^0)) = 3.3 \text{ GeV}$$

$$\Delta\sin^2\theta = 0.014 \Rightarrow \Delta(M(Z^0)) = 2.4 \text{ GeV}$$

$$\text{from UA1 and UA2} \Rightarrow \Delta(M(Z^0)) = 2.5 \text{ GeV}$$

demonstrating the need for higher precision measurements.

The future improvements to the luminosity of the collider (ACOL project) are expected to boost the integrated luminosity from 100 nb^{-1} to 10000 nb^{-1} The improvement to be expected in the measurements of $\sin^2\theta$ can be estimated for the two equations by which $\sin^2\theta$ can be determined from the masses.

- From $\sin^2\theta = 1 - M(W)^2/M(Z^0)^2$: In this expression the absolute mass scale drops out, and probably other systematic effects are small. One could expect an improvement of the order of the improvement in the statistical error. Hence, a precision $\Delta\sin^2\theta = \pm 0.004$ can be expected.
- From $\sin^2\theta = A^2/M(W)^2$: For higher statistics the result from this expression will be dominated by the scale error on the mass measurement. If one assumes that the absolute calibration of these big calorimeters can be performed to 1% one derives a limiting accuracy of $\Delta\sin^2\theta = \pm 0.004$.

Having these future improvements to the direct mass measurements in mind these can serve as a goal to be reached by the $\sin^2\theta$ measurements in other processes. At present there are several attempts to reach a precision of $\Delta\sin^2\theta = \pm 0.005$ in neutrino scattering, some of them will be discussed in the following sections.

4. HIGH PRECISION SEMI-LEPTONIC NEUTRINO MEASUREMENTS

It was shown by Llewellyn-Smith that for isoscalar targets the major contributions to the NC and CC cross-sections are related by assuming isospin invariance alone [6]. The following equation for the differential cross-sections applies:

$$d^2\sigma_{NC}^{\nu(\bar{\nu})}/dxdy = (1/2-\sin^2\theta+5/9\sin^4\theta)\ d^2\sigma_{CC}^{\nu(\bar{\nu})}/dxdy + (5/9\sin^4\theta)\ d^2\sigma_{CC}^{\bar{\nu}(\nu)}/dxdy \qquad (3)$$

Integrating eq. (3) over x and y one obtains a relation containing only ratios of total cross-sections. The measurement sensitive to $\sin^2\theta$ is the ratio of of neutral-current over charged-current total cross-sections for neutrinos, R_ν.

At present two goups at CERN are analysing data taken in 1984 to measure R_ν with high precision. An upgraded version of the narrow-band beam is used at 160 Gev central momentum with nearly a factor two more flux than previously. The method used by the two groups is completely different, and a comparison of the results will provide a good test of the systematic uncertainties involved. The experimental parameters are summarized in Table 5. In the following sections the CHARM experiment will be described in some detail.

Table 5: Comparison of high precision R_ν measurements.

	CDHS [7]	CHARM [8]
beam	160 GeV NBB	160 GeV NBB
statistics CC	250,000	120,000
NC	80,000	40,000
E_H-cut	10 GeV	2 GeV
p_μ-cut	≈ 3 GeV	1 GeV
method	event-length	muon-recognition
total corr.	≈ 25 %	≈ 15 %
$\Delta\sin^2\theta$	0.005	0.005

(not including common theoretical error)

4.1 The experimental set up

The CHARM neutrino detector is a fine-grain calorimeter followed by an iron spectrometer with a toroidal magnetic field, and surrounded by a magnetized iron frame. The calorimeter has a sampling corresponding to one radiation length, with scintillators, proportional drift tubes and streamer tubes as

detecting elements. It is described in detail elsewhere [9]. A view of the CHARM-I detector is shown in fig. 1. The fiducial mass used in this exposure was 87 tons.

Data were taken in the 160 GeV narrow band beam (NBB), developed by Grant and Maugain [10] as a high flux version of the CERN NBB optics. It satisfies the conditions for a precision measurement of R_ν, namely [11]

- A sufficiently high average neutrino energy, needed for efficient pattern recognition in the CHARM detector.
- Low background contributions, measurable with high accuracy.
- The possibility to measure the relative $\bar{\nu}/\nu$ flux normalization accurately.
- A calculable neutrino energy spectrum.
- A high event rate.

In addition to these points it posseses a well-defined energy-radius correlation of the neutrino flux. This makes it possible to obtain y-distributions of neutral-current interactions.

4.2 Event classification and corrections

Interactions in the CHARM detector are classified by an automatic pattern-recognition program on an event-by-event basis. Selection criteria are applied which attempt to identify optimally the physical processes and to minimize the corrections needed to relate the visible cross-sections to the physical cross-sections.

Neutrino interactions are defined as events without entering charged tracks. A neutrino event is called a charged-current interaction if it contains a muon originating from the event vertex. The muon has to be visible over a range corresponding to an energy-loss of at least 0.67 GeV. Its total range has to exceed 1 GeV energy-loss. All other neutrino-event candidates

are classified as neutral-current interactions. Only those events which have their vertex inside the fiducial volume and which have a shower energy of at least 2 GeV are analysed. An off-line representation of an NC and CC event in the CHARM-detector are shown in fig. 2 and 3.

The following corrections have to be applied to obtain the CC and NC event numbers:

The classification efficiency of the automatic pattern recognition is known to be better than 99.5%. In addition, a flag is generated by the program to tag situations where the automatic procedure could fail. A visual inspection of these flagged events (~ 4000) together with a scan of a randomly selected sample of events reduces the error introduced by classification errors to $\Delta R_\nu/R_\nu \leq 0.1\%$.

CC events in which the primary muon cannot be identified are classified as NC. The majority of these muons have an energy less than 1 GeV. A smaller contribution to the loss of CC events is caused by muons of more than 1 GeV either leaving the sides of the detector before their energy loss is sufficiently large, or by muons obscured by the hadronic shower. The total correction induced by all sources of unidentified muons is of the order of 2% of the CC event rate, and induces an uncertainty amounting to $\Delta R_\nu/R_\nu \approx 0.3\%$.

A small fraction of NC events contains a track which fulfils the requirements of a primary muon of a CC event, and which are classified as CC events. This background is caused by decays of pions or kaons in the shower or by punch-through tracks. The size of this correction is of the order of 2%, giving $\Delta R_\nu/R_\nu \approx 0.2\%$.

Both the NC and CC interactions of electron neutrinos originating from K_{e3}-decays in the beam are classified as NC events. The contribution of these

events amounts to ~ 5% of the NC candidates (~ 2% in the $\bar{\nu}$ exposure). With a measurement of the K/π ratio with an accuracy of ~ 2 ÷ 3%, this correction can be calculated to ± 5% of its value, corresponding to $\Delta R_\nu/R_\nu \simeq 0.4\%$.

The flux from decays before the decay tunnel is not well calculable, and has to be subtracted using data obtained with the entrance of the decay tunnel blocked by an absorber. The uncertainty introduced by this wide-band (WB) background amounts to $\Delta R_\nu/R_\nu \simeq 0.3\%$.

The uncertainty introduced by the cosmic-ray background during normal data taking is small, because sufficient data can be taken in periods without beam to measure the correction and because the correction is rather small.

The final experimental precision obtained in the measurement of R_ν is summarized in Table 6.
The uncertainty in r is dominated by the event-statistics (1.5%), WB background subtraction (1.5%) and relative normalization error of the $\bar{\nu}$ to the ν flux (2.0%). A 3% accuracy in r is therefore expected. The accuracy of the measurements of R_ν and r as given above is sufficient to ensure an experimental precision $\Delta\sin^2\theta = \pm 0.005$.

4.2.1 Theoretical uncertainty in $\sin^2\theta$

At this level of experimental precision it is worthwile to consider the uncertainties introduced by the interpretation of R_ν in terms of $\sin^2\theta$. The main contributions to the theoretical error can be classified as follows:

- Uncertainties in the Kobayashi-Maskawa (K.M.) mixing matrix.
- The momentum-weighted content of s and c quarks in the nucleon, and threshold-effects in c-production.
- Higher twist terms.

Table 6: Error Sources in the Measurement of R_ν

Error source	% error in R_ν
statistics	0.7%
Classification inefficiencies	0.1%
WB background + cosmic	0.3%
μ recognition losses	0.3%
π/K decays in the shower	0.2%
K_{e3} decays	0.4%
Total systematic error	0.7%
Total error	1.0%

A careful analysis [6] of the uncertainties shows that, using eq. (3), the uncertainty is $\Delta\sin^2\theta(\text{theory}) \cong 0.01$. If in addition it is assumed that the matrix is almost diagonal, this error is reduced to $\pm$ 0.005. An additional uncertainty due to higher twist terms is estimated to be smaller than 0.005 [6].

However, if one uses other methods such as the Paschos-Wolfenstein relation

$$R^- = \frac{\sigma_{NC}^{\nu} - \sigma_{NC}^{\bar{\nu}}}{\sigma_{CC}^{\nu} - \sigma_{CC}^{\bar{\nu}}} = (1/2) - \sin^2\theta$$

one obtains a smaller theoretical uncertainty, by cancelling the sea contributions. This methods requires more antineutrino data to obtain the same statistical accuracy. Since the event rates in antineutrino beams are usually a factor six lower per incident proton, the small statistics in the antineutrino measurements determine the final accuracy.

4.3 The measurement of $\sin^2\theta$ using the y-distributions

An alternative method was proposed, relying on comparisons of the y-distributions of neutral-current and charged-current neutrino and antineutrino interactions [12]. The uncertainties proportional to the strange quark component in the nucleon can be removed by exploiting the additional information provided by a simultaneous measurement of the NC and CC y-distributions of neutrino and antineutrino scattering. The normalization of the ill-known terms can be introduced as free parameters. Corrections for the s-quark contributions to the NC cross-sections are treated by the substitution:

$$d\sigma_{NC}/dy \rightarrow d\sigma_{NC}/dy - (g_s^2 \cdot s) \cdot f(y) \qquad (4)$$

where $(g_s^2 \cdot s)$ is a free parameter and $f(y)$ is obtained using a specific model, e.g. in the scaling limit

$$f(y) \rightarrow 2(1+(1-y)^2) \qquad (5)$$

The free parameter $(g_s^2 \cdot s)$ is interpreted as being the product of the coupling of the weak neutral-current to the strange quark, g_s^2, and the strange quark content of the nucleon, s. This model can be improved by using parametrizations including quantum-chromodynamic (QCD) type corrections. In the charged-current sector a similar correction is made, based on di-muon measurements:

$$d\sigma_{CC}/dy \rightarrow d\sigma_{CC}/dy - B^{-1}\, d\sigma_{di\text{-}\mu}/dy \qquad (6)$$

in which B (the average branching ratio to muons of charm states produced in this process) is a free parameter. This procedure takes care of threshold effects and removes any need for a priori knowledge on the product of the element $|U_{cs}|^2$ and the absolute strange quark component in the nucleon.

The corrections which remain to be applied involve the knowledge of the mixing elements $|U_{ud}|$, $|U_{us}|$, $|U_{cd}|$, and the contribution of charm quarks to the NC and CC cross-sections. According to Llewellyn-Smith [6] these corrections are calculable to within an uncertainty of $\Delta\sin^2\theta = \pm 0.004$. No assumptions on the shape of the parton distributions other than eq. (5) or its equivalent have to be made.

This method improves on previous determinations of $\sin^2\theta$ from the differential cross-sections $d\sigma/dy$ because it uses the quark-parton model in correction terms only and, therefore, scaling violations and threshold effects are taken into account intrinsically. The influence of higher twist effects can be shown to be small ($\Delta\sin^2\theta < \pm 0.005$ [6]).

4.4 The measurement of the y-distribution

The fine granularity of the CHARM calorimeter not only permits a powerful separation of NC and CC induced events, but also a precise measurement of the vertex and energy of hadronic showers [13]. These features, together with the energy-radius correlation of the NBB, make a measurement of the y-distribution of NC events possible [14].

The statistical accuracy of $\sin^2\theta$ as obtained from the y-distributions is mainly determined by the neutrino statistics, but also some antineutrino data

is needed. A fit to the y-distributions, including the contributions of strange quarks to the CC and NC cross-sections as free parameters, provides a statistical uncertainty of $\Delta\sin^2\theta$ (statistical) = ± 0.006. The experimental systematic uncertainty is estimated to be $\Delta\sin^2\theta$ (systematic) = ± 0.003.

Table 7 summarizes the different errors in the various methods for an exposure yielding 100,000 neutrino CC events and 10,000 antineutrino CC events.

Table 7: $\Delta\sin^2\theta$ with different methods.

error type	from R_ν	from P.W. relation	from $d\sigma/dy$
statistical	0.0035	0.008	0.006
systematic	0.0035	≈ 0.0035	≈ 0.0035
theoretical	0.01	0.003	0.004

5. NEUTRINO-ELECTRON SCATTERING

The advantage of using a purely leptonic process to determine $\sin^2\theta$ is clearly shown by the discussion on theoretical errors in the semi-leptonic case. This process is fully understood theoretically, and the measurement is a purely experimental problem. The cross-sections of muon-neutrino electron scattering can be written in terms of the vector and axial vector coupling of the electron, g_V^e and g_A^e, as follows:

$$\sigma(\nu_\mu e \to \nu_\mu e) = G^2 m_e E_\nu / 2\pi \{ (g_V^e + g_A^e)^2 + (1-y)^2 (g_V^e - g_A^e)^2 \}$$
$$\sigma(\bar{\nu}_\mu e \to \bar{\nu}_\mu e) = G^2 m_e E_\nu / 2\pi \{ (g_V^e - g_A^e)^2 + (1-y)^2 (g_V^e + g_A^e)^2 \}$$

where $y = E_e/E_\nu$, the ratio of the recoil electron energy and the incident neutrino energy and m_e the electron mass. The low cross-section of the elastic scattering of muon-neutrinos on electrons compared to the inclusive semi-leptonic cross-section, $\sigma(\nu_\mu e) \approx 10^{-4}\ \sigma(\nu_\mu N)$, presents a formidable experimental problem. The experimental tools involve a good electron-pion separation, some electron-photon separation and a measurement of the recoil electron angle, θ_e, in large-mass detectors.

A sensitive measurement of $\sin^2\theta$ can be obtained using the ratio of neutrino and antineutrino cross-sections:

$$R = \frac{\sigma(\nu_\mu e)}{\sigma(\bar{\nu}_\mu e)} = \frac{1 + \eta + \eta^2}{1 - \eta + \eta^2} \qquad (7)$$

where $\eta = 1 - 4 \sin^2\theta$. From equation (7) follows $\Delta\sin^2\theta \cong (1/8)\ \Delta R/R$ for $\sin^2\theta$ close to 0.25. The use of this ratio has also experimental advantages if it is measured with a single apparatus since

- the efficiencies for finding electrons cancel;
- some of the systematic uncertainties in the background subtraction cancel; and
- no absolute normalization of the neutrino fluxes is needed, since only the ratio of neutrino and antineutrino fluxes enters.

Measurements of $\sin^2\theta$ using the method of the ratio of the cross-sections were first obtained by the CHARM-collaboration [15]. The results are summarized in the following section. A measurement with similar precision was reported recently by the E734 collaboration at Brookhaven [16]. On the basis of the experience with the CHARM-I detector a new dedicated detector is being built, with the aim to provide a precision $\Delta(\sin^2\theta) \cong 0.005$.

5.1 The CHARM-I $\nu_\mu e$ scattering experiment

The CHARM-collaboration has obtained 83 $\nu_\mu e$ scattering events and 112 $\bar{\nu}_\mu e$ scattering events in the CERN wide band beam (WBB).

Events of electromagnetic nature are selected on the basis of their shower properties, rejecting the background by a factor $\cong$ 300. Events were selected requiring:

- a small energy deposition in the first scintillator plane (E_F) not exceeding seven minimum ionizing particles;
- the number of wires hit in the proportional and streamer tube planes following the vertex to be small;
- a small width of the shower, as shown in fig 4.

The measurement of the recoil electron angle reduces the backgrounds further by exploiting the kinematics of the process: $E_e\theta_e^2 \leq 2m_e$, which provides a signal peaking in the forward region, while the backgrounds have much broader angular distributions. The results are shown in fig. 5. The remaining backgrounds are composed of ν_e quasi-elastic interactions and ν_μ neutral-current interactions, including coherent π^0 production. The relative amount of the two background components was evaluated from the study of the E_F distribution shown in figure 6; they are different for showers initiated by electrons, photons or neutral pions.

The neutrino and antineutrino fluxes were measured by analysing events induced by quasielastic charged-current scattering on nucleons [17] and the events induced by inclusive neutral- and charged-current processes on nucleons [18]. The ratio of the normalized numbers of $\nu_\mu e$ and $\bar{\nu}_\mu e$ events is found to be

$$R_{exp} = N(\nu_\mu e)/N(\bar{\nu}_\mu e) \times F = \sigma(\nu_\mu e)/\sigma(\bar{\nu}_\mu e) = 1.26 \; {}^{+0.41}_{-0.28}$$

The flux factor, F, was obtained by taking the average of both flux determinations. The relation between R_{exp} and $\sin^2\theta$ given by eq. (7) is shown in figure 7. One obtains:

$$\sin^2\theta = 0.215 \pm 0.032 \text{ (stat)} \pm 0.012 \text{ (syst)}.$$

In fig. 8 the allowed areas in the g_V-g_A plane are shown. Four regions are allowed by $\nu_\mu e$ and $\bar{\nu}_\mu e$ scattering. Combining these regions with electron-positron annihilation data and electron-neutrino-electron scattering results one solution survives:

$$g_A^e = -0.54 \pm 0.05 \text{ (stat)} \pm 0.06 \text{ (syst)}$$
$$g_V^e = -0.08 \pm 0.07 \text{ (stat)} \pm 0.03 \text{ (syst)}$$

Using the absolute value of the cross-section determinations, the relative strength of the neutral- and charged-current coupling constants is found to be

$$\rho = 1.09 \pm 0.09 \text{ (stat)} \pm 0.11 \text{ (syst)},$$

in agreement with the prediction of the standard model.

5.2 The CHARM-II detector

The CHARM-II detector is being built at CERN and is approved for an exposure corresponding to 2000 events in each channel, aiming at an accuracy $\Delta\sin^2\theta = 0.005$ [20]. This detector is expected to be fully operational in 1986. The techniques used here are extrapolated from the experience obtained with the CHARM-I detector. The main improvements with respect to the CHARM-I detector are:

- A finer granularity both longitudinally and laterally, in order to achieve a higher efficiency for selecting electron showers as well as a better angular resolution for electron showers by a factor three, reducing the total background by a factor five.
- A five-fold increase in fiducial mass.
- An optimized performance of the wide-band neutrino beam.

The structure of the detector is sketched in figure 9. It consists of 420 equal units of 3.7 x 3.7 m^2 surface area, each composed of a 5 cm thick glass plate and of a plane of streamer tubes with 1 cm wire spacing, read out by the wires and by cathode strips of 2 cm spacing, perpendicular to the wires. The wires are readout digitally to obtain unambiguous information about the track multiplicity near the vertex. The signal from the strips is read out with analogue electronics and provides a ± 2 mm accuracy of the centroid position of a track, and a precise measurement of the position of the shower core. A simulation of this detector by Monte Carlo methods gives an electron shower angular resolution of $\sigma(\theta) \sim 16$ mrad/$\sqrt{E/GeV}$, similar to the natural angular spread of recoil electrons in this process. The signal to background ratio is expected to improve by a factor of five. An exposure with $1.5 \cdot 10^{19}$ protons will yield ~ 2000 events in each channel.

Monitoring of the neutrino flux and of the beam composition using quasi-elastic events has been studied in detail by the CHARM-I experiment. A total flux ratio error of ± 2% is estimated, leading to a total error of ± 4%

on R, and a corresponding experimental error of $\Delta\sin^2\theta = \pm 0.005$. There is no theoretical uncertainty in extracting this result from the data.

6. SUMMARY

The present experimental status supports the low energy predictions of the standard model. However, to obtain a meaningful test of the loop-level corrections it is needed to improve the experimental precision. This precision will be reached by two semileptonic neutrino-scattering experiments performed in 1984 at CERN. However the present theoretical uncertainty in the interpretation of these experiments are still too large. A determination of $\sin^2\theta$ using a purely leptonic process does not suffer from these uncertainties. The CHARM-II detector is being built at CERN aiming at a precision in $\sin^2\theta$ to give meaningful tests of the first order corrections of the theory. These neutrino experiments will match the precision reached in the near future with the direct mass-measurements obtained at the Sp$\bar{p}$S collider at CERN, upgraded with the ACOL project.

7. REFERENCES

1. Hasert, F.J. et al.. 1973. Phys. Lett. B46: 138.
2. Glashow, S.L.. 1961. Nucl. Phys. 22: 579; Salam, A. and J. Ward. 1964. Phys. Lett. 13: 168; Weinberg, S. 1964. Phys. Rev. Lett. D5: 1264.
3. Panman, J. 1984. XIth International Conf. on Neutrino Physics and Astrophysics, Dortmund, and references therein.
4. Arnison, G. et al. 1983. Phys. Lett. B122: 103; Phys. Lett. B126: 398; Phys. Lett. B129: 273; Banner, M. et al. 1983. Phys. Lett. B122: 476; Bagnaia, P. et al. 1983. Phys. Lett. B129: 130.

5. Marciano, W.1983. proc. Int. Lepton and Photon Symp, Cornell; Marciano, W. and A. Sirlin. 1983. Testing the standard model by precise determinations of W and Z masses, BNL preprint.

6. Llewellyn-Smith. 1983. C.H., Contribution to Fixed Target Workshop, CERN, 1982; Nucl. Phys. B228: 205-215.

7. Dydak, F. et al. 1983. CERN/SPSC/83-49.

8. Bergsma, F. et al. 1984. CERN/SPSC/84-1.

9. Diddens, A.N. et al. 1978. Nucl. Instr. & Meth. 157: 35; and Jonker, M. et al. 1982. Nucl. Instr. & Meth., 200: 183.

10. Grant, A. and J.M. Maugain. 1983. CERN/EF/BEAM 83-2.

11. Panman, J. 1982. Contribution to the SPS Fixed Target Workshop, CERN.

12. Panman, J. 1984. CERN-EP/84-172, to be published In Phys. Lett. B.

13. Abt, I. et al. 1983. Nucl. Instr. & Meth. 217: 377-381.

14. Jonker, M. et al. 1981. Phys. Lett. B102: 67.

15. Jonker, M. et al. 1982. Phys. Lett. B117: 272; Bergsma, F. et al. 1984. Phys. Lett. B147: 481.

16. Ahrens, L. A. et al. 1985. Phys. Rev. Letters 54: 18.

17. Jonker, M. et al. 1980. Phys. Letters B93: 203; Bergsma, F. et al. 1983. Phys. Letters B122: 465.

18. Jonker, M. et al. 1981. Phys. Lett. B99: 265.

19. Reines, F. , H.S. Gurr and H.W. Sobel. 1976. Phys. Rev. Lett. 37: 315; the limits shown in figure 8 have been evaluated by Krenz, W. 1982. RWTH Aachen, Pitha 82/26.

20. Busi, C. et al. 1983. CERN/SPSC/83-24 and 83-37.

8. FIGURE CAPTIONS

fig. 1. Photograph of the CHARM-detector.

fig. 2. Off-line representation of a neutral-current event recorded in the CHARM-detector.

fig. 3. Off-line representation of a charged-current event recorded in the CHARM-detector.

fig. 4. Width, Γ, of showers induced by electrons and pions measured in a test beam with the CHARM-I detector.

fig. 5. $E^2\theta^2$ distributions for (a) neutrino, (b) antineutrino events; in (c) and (d) the additional condition $E_F < 8$ MeV is applied.

fig. 6. Distribution of E_F (energy deposition in the first scintillator plane following the vertex) for (a) electrons and (b) π^0.

fig. 7. Relation between $R = \sigma(\nu_\mu e)/\sigma(\bar{\nu}_\mu e)$ and $\sin^2\theta$ with the measured value of R and the corresponding value of $\sin^2\theta$.

fig. 8. Values of g_A^e and g_V^e the neutral current coupling constants obtained from measurements of $\sigma(\nu_\mu e)$ and $\sigma(\bar{\nu}_\mu e)$ by the CHARM Collaboration [15]. The limits from forward-backward asymmetry in $e^+e^- \rightarrow \ell^+\ell^-$ (see e.g. [3]) and from $\sigma(\bar{\nu}_e e)$ measurements [19] select a unique solution.

fig. 9. Sketch of the structure of the CHARM-II detector.

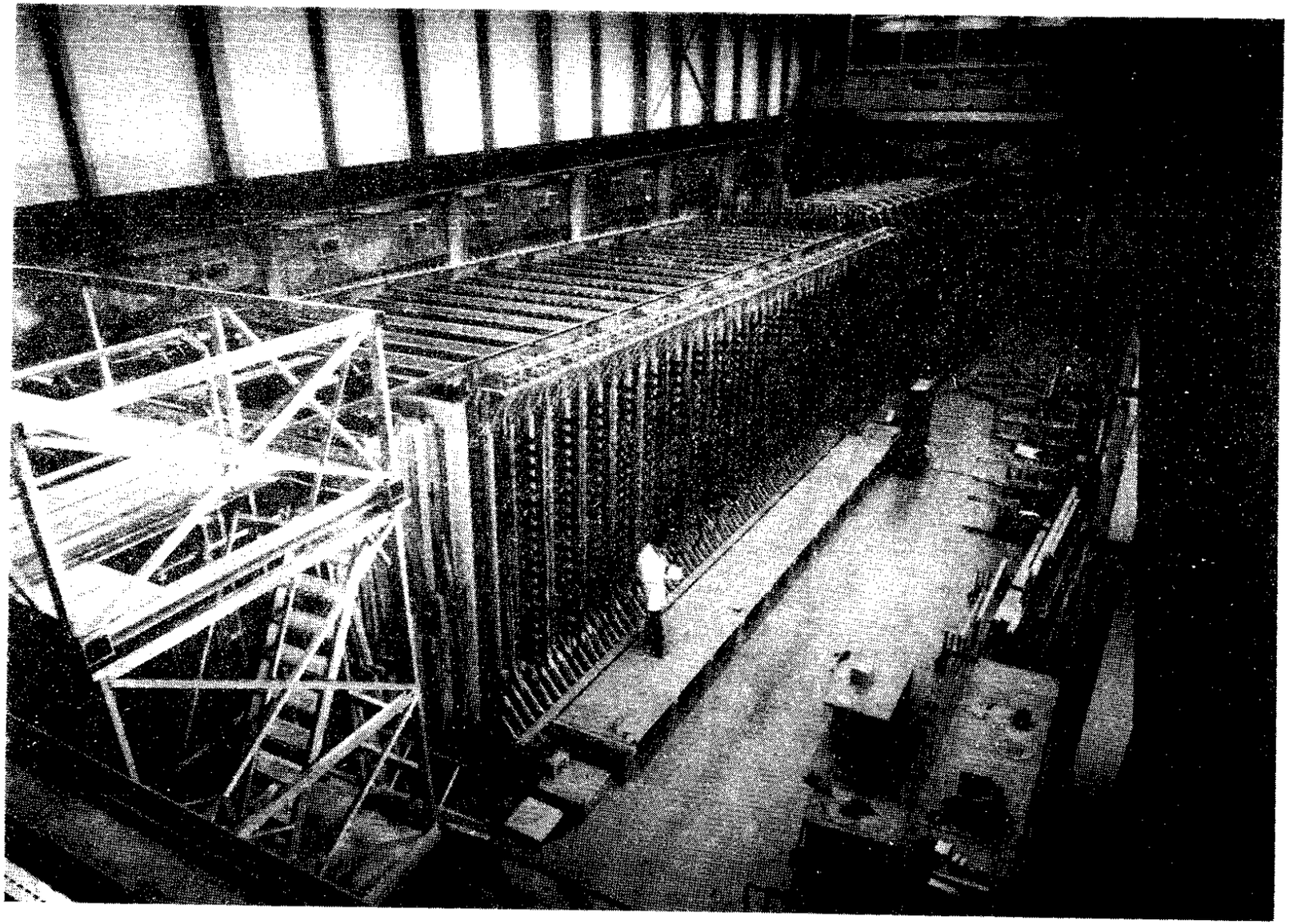

fig. 1.

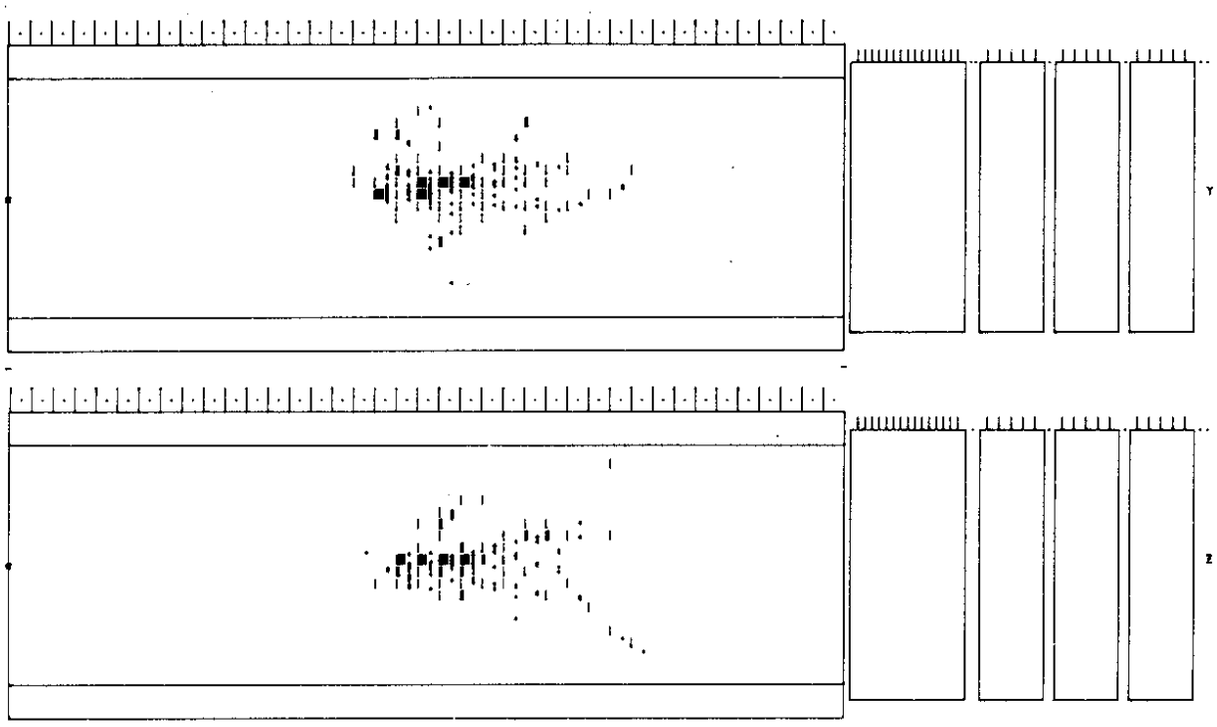

fig. 2.

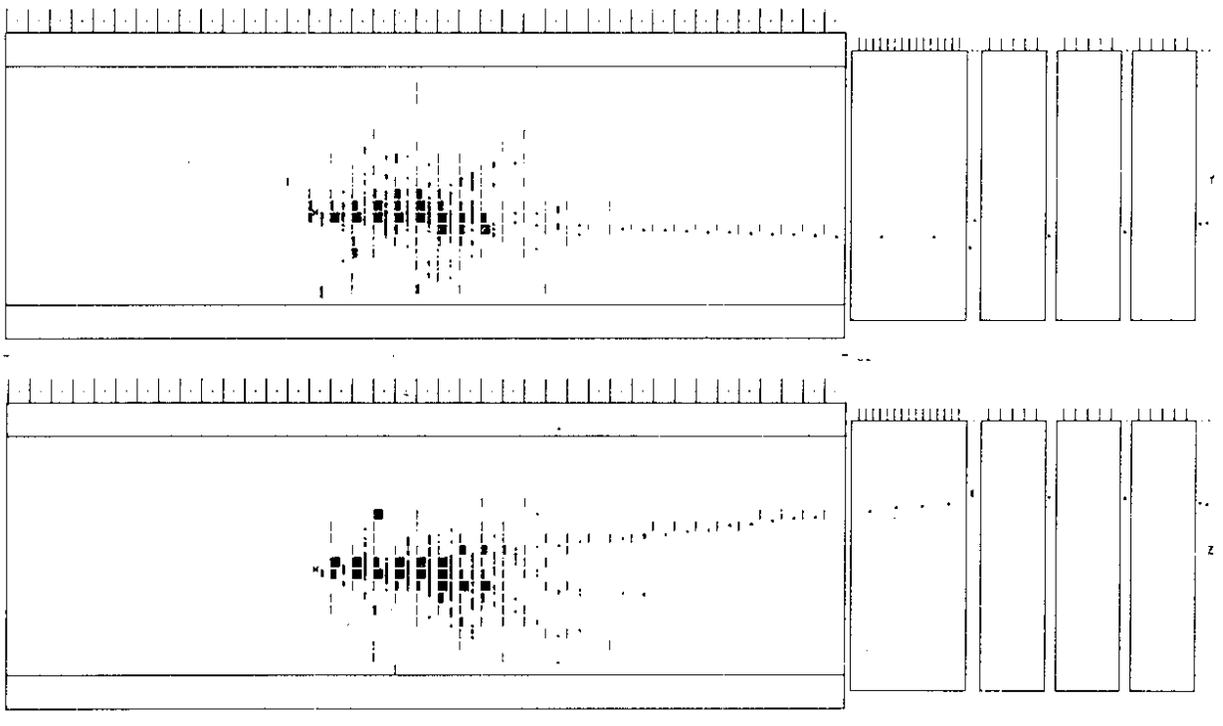

fig. 3.

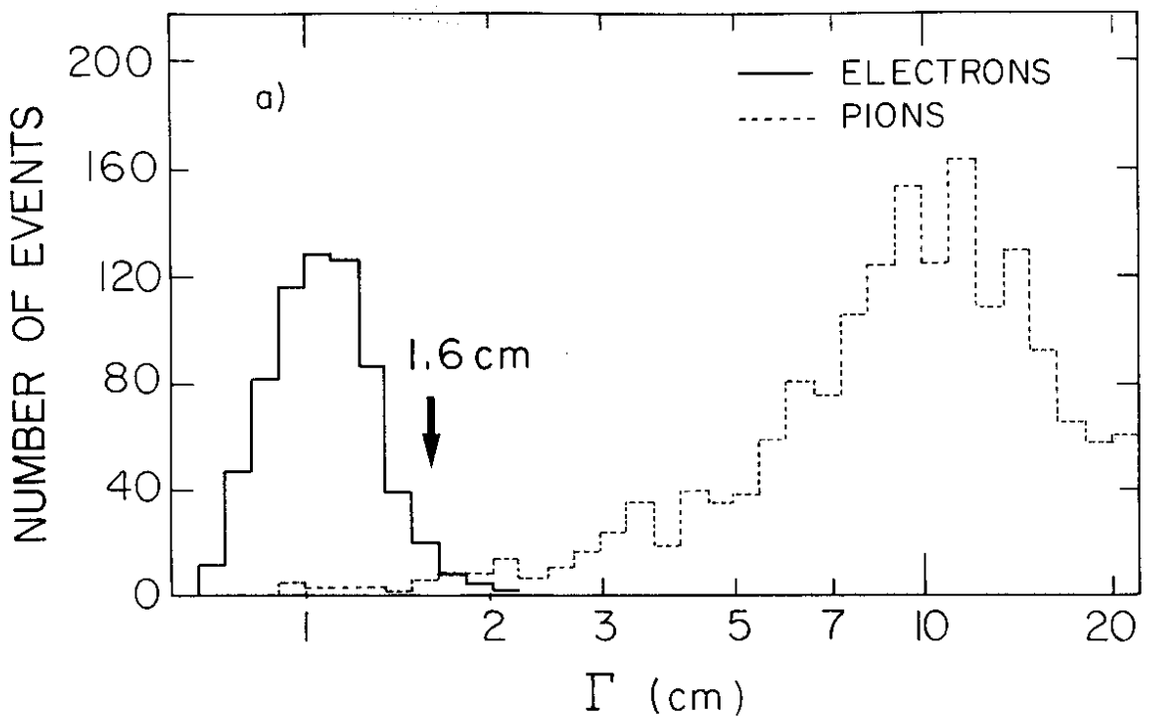
a)
ELECTRONS
PIONS
1.6 cm
NUMBER OF EVENTS
200
160
120
80
40
0
1
2
3
5
7
10
20
Γ (cm)

fig. 4.

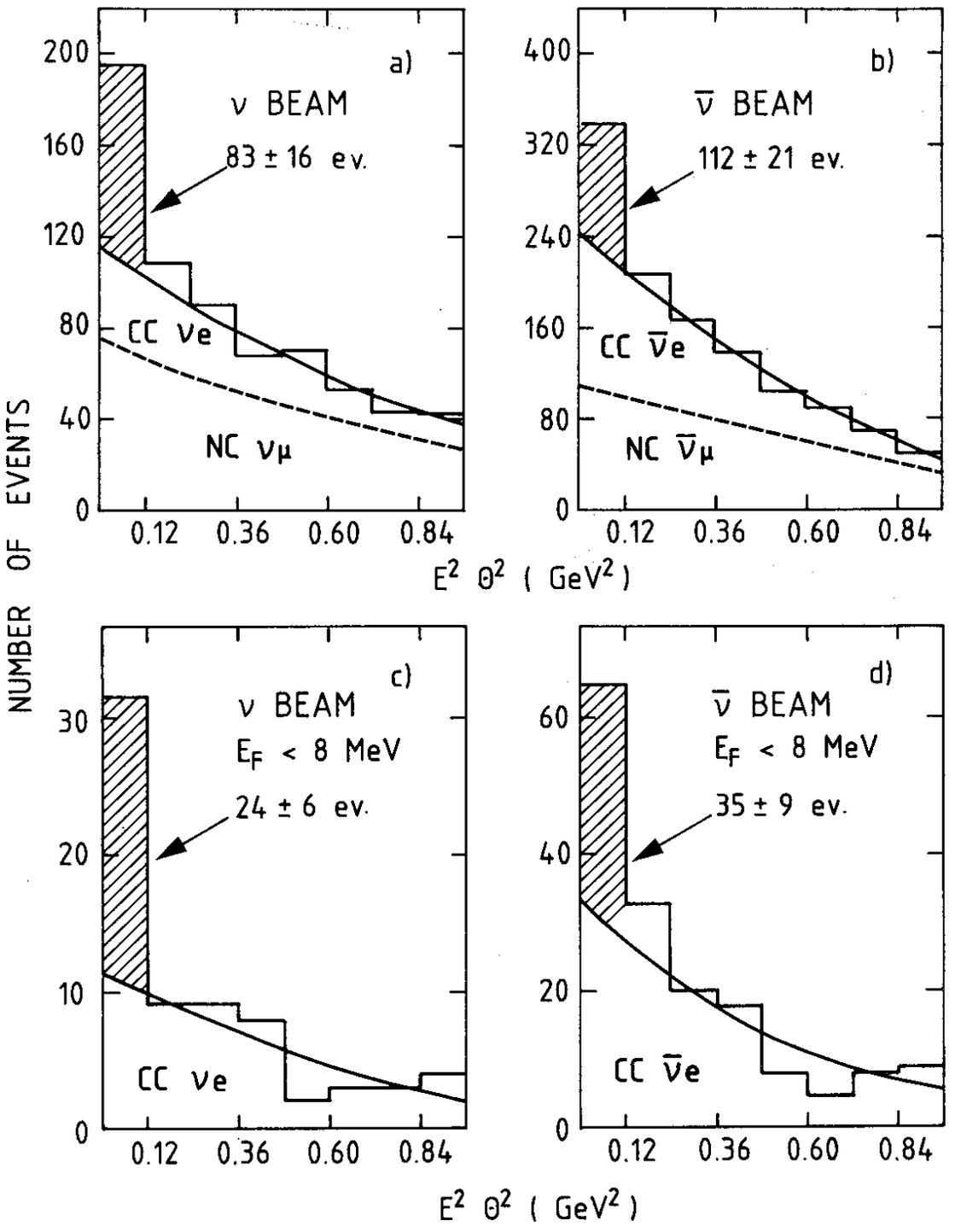
a)
ν BEAM
83 ± 16 ev.
CC νe
NC νμ
b)
ν̄ BEAM
112 ± 21 ev.
CC ν̄e
NC ν̄μ
c)
ν BEAM
E_F < 8 MeV
24 ± 6 ev.
CC νe
d)
ν̄ BEAM
E_F < 8 MeV
35 ± 9 ev.
CC ν̄e
NUMBER OF EVENTS
E² θ² (GeV²)
0.12
0.36
0.60
0.84

fig. 5.

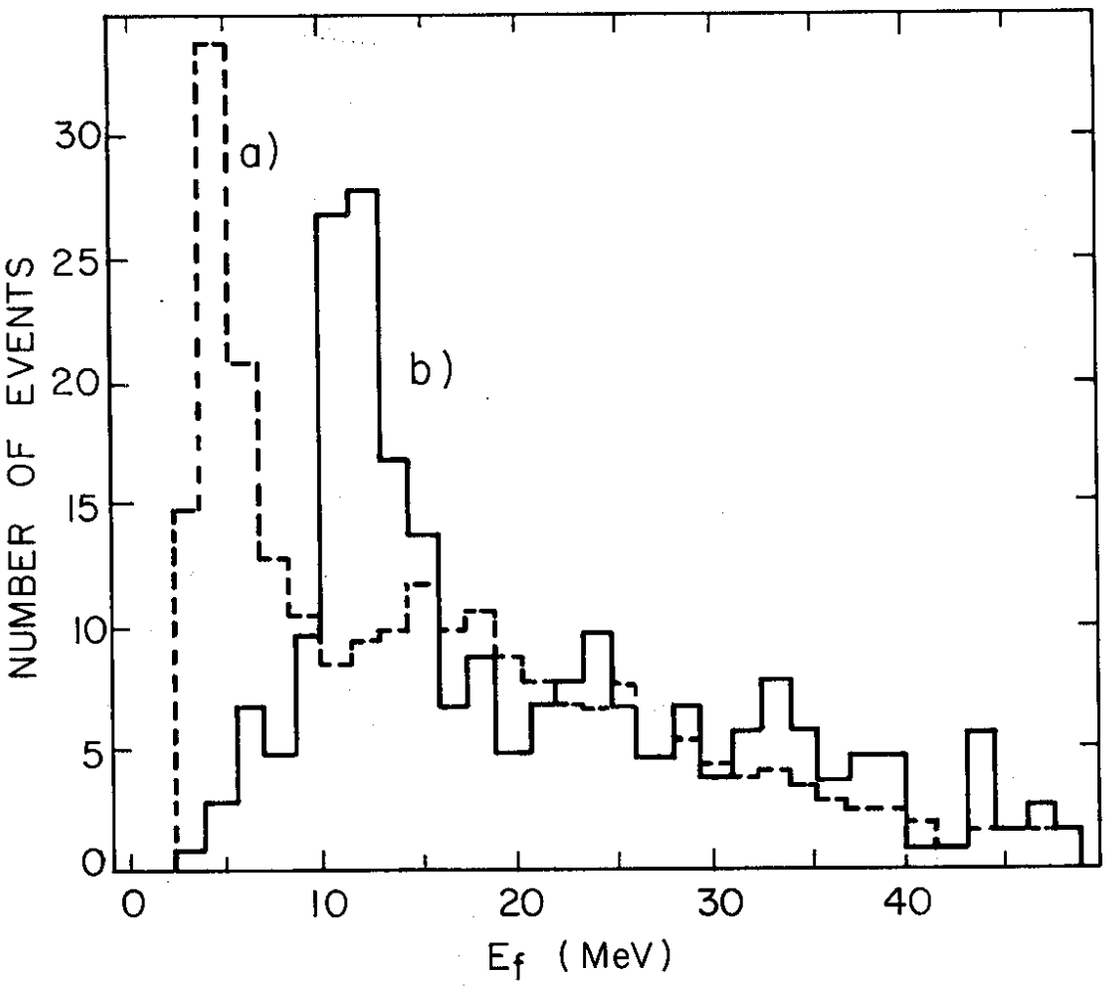

fig. 6.

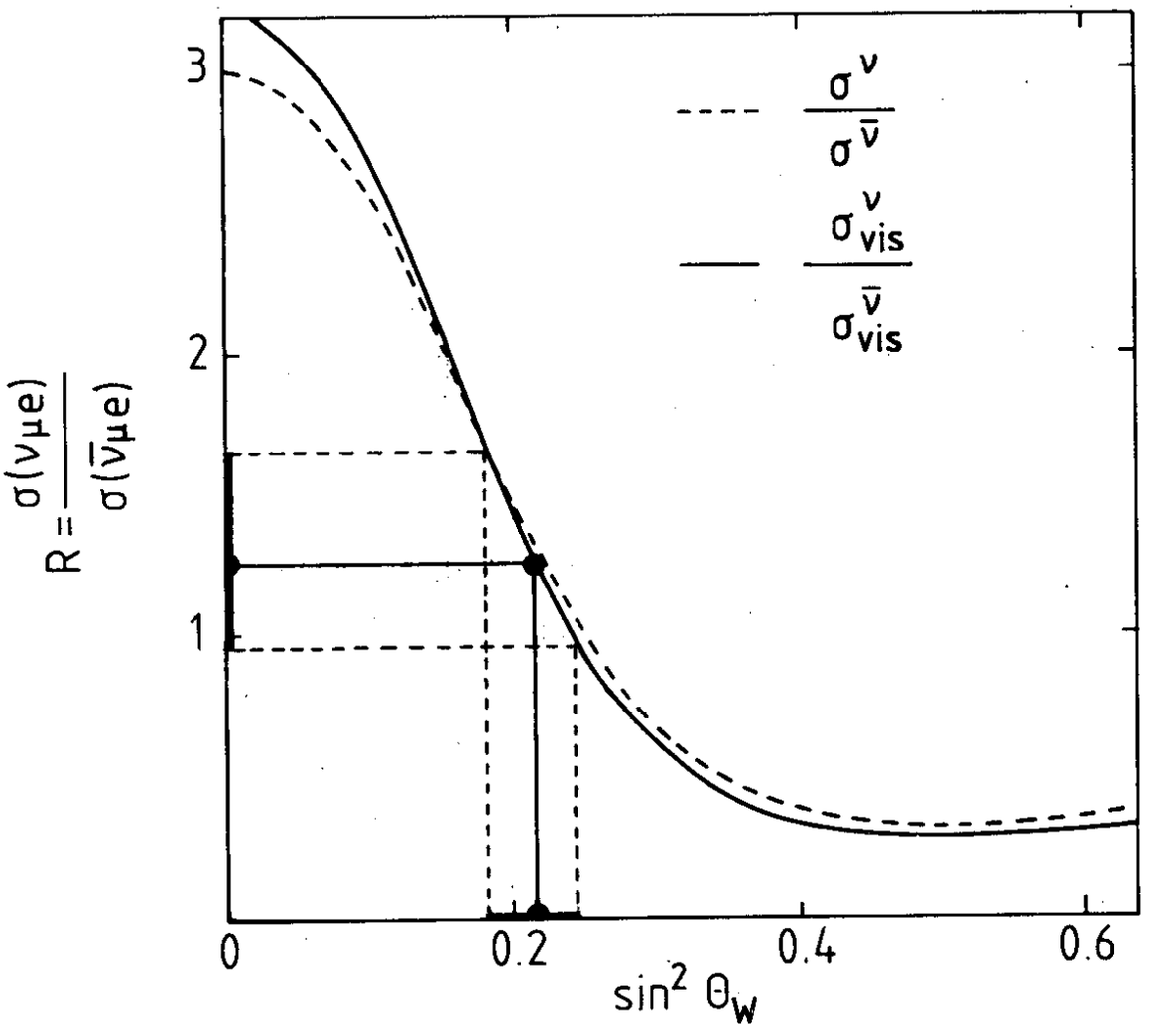

fig. 7.

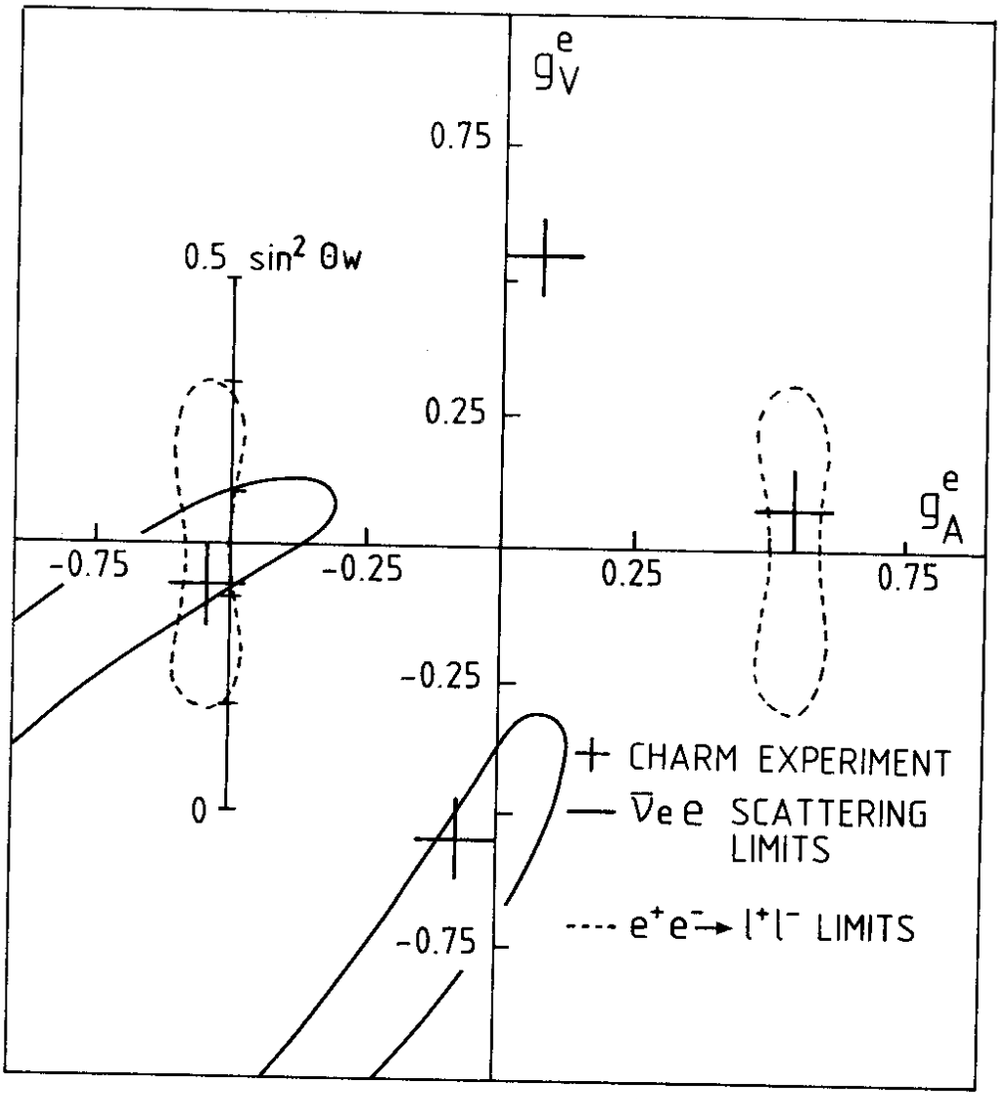
g_V^e
0.75
0.5 $\sin^2 \theta_W$
0.25
g_A^e
-0.75
-0.25
0.25
0.75
-0.25
0
-0.75
CHARM EXPERIMENT
$\bar{\nu}_e e$ SCATTERING LIMITS
$e^+e^- \rightarrow l^+l^-$ LIMITS

fig. 8.

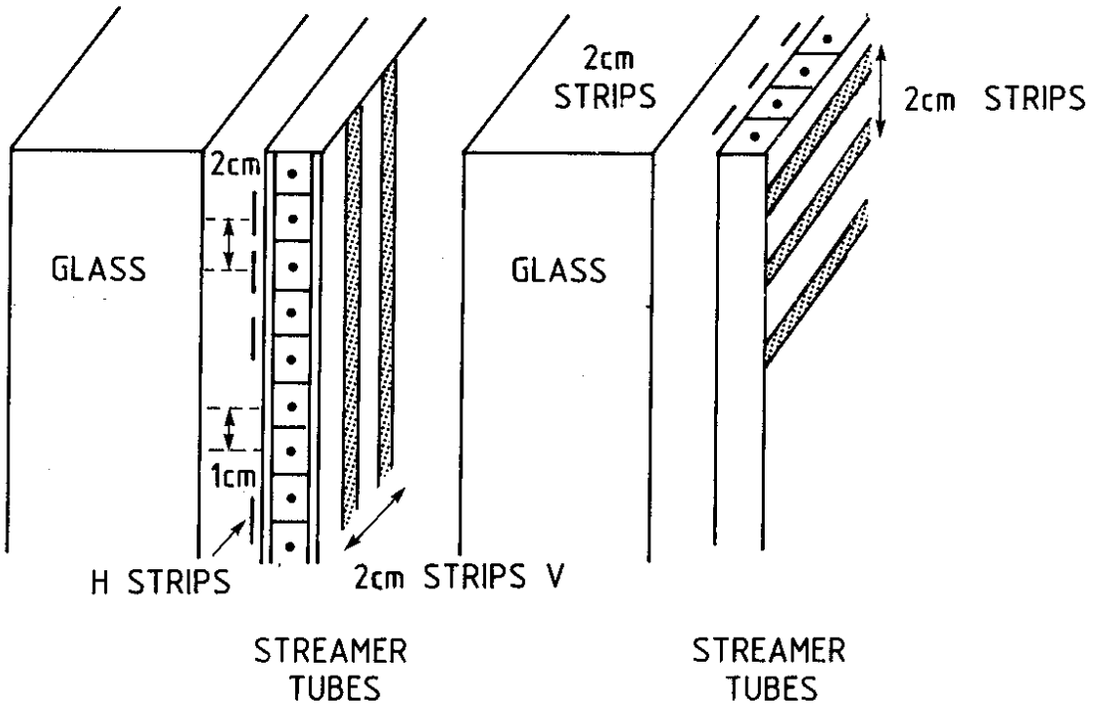
2cm
STRIPS
2cm STRIPS
GLASS
2cm
GLASS
1cm
H STRIPS
2cm STRIPS V
STREAMER
TUBES
STREAMER
TUBES

fig. 9.